INVESTIGATION REPORT ET/IR 511R

AN EVALUATION OF THE USE OF AIRBORNE
INFRA-RED THERMOGRAPHY AS A METHOD FOR
MONITORING SPONTANEOUS COMBUSTION
AND GREENHOUSE GAS EMISSIONS

ACARP PROJECT C9062

J N Carras, S J Day, F Szemes, *J A Watson & D J Williams

CSIRO Energy Technology
PO Box 136, North Ryde NSW 1670

*Watson Mining Management
PO Box 204, Muswellbrook NSW 2333

June 2002

SUMMARY AND OUTCOMES

Objectives:

The principal objectives of project C9062 were to:

1. develop a method for estimating and monitoring the extent of spontaneous combustion in open cut coal mines using airborne infra-red thermography and

2. use the temperature data from the infra-red surveys to estimate greenhouse gas emissions from spontaneous combustion.

Methodology

The original work program for the project consisted of two thermal infra-red flights to be carried out, one in the Hunter Valley the other in the Bowen Basin. This work program was modified during 2001 so that the two flights were held in the Hunter Valley. The reasons for this were due to issues that had arisen during the processing of the data from the first flight. The second flight was carried out over similar ground in the Hunter Valley in order to:

a) provide a comparison with the data obtained during the first flight so as to address any issues that might arise from a direct comparison

b) provide data at greater resolution than the first flight to investigate the significance of large cracks in the spoil from which large emissions of hot gases could be emanating

Three flights were carried out as follows.

Flight	Pixel size
September 2000	7x7 m
October 2001	7x7 m
October 2001	2x2 m

A significant amount of data was also to be obtained using the CSIRO chamber to measure surface emissions so as to establish the clearest possible relationship between greenhouse gas emissions and surface temperature of hot spoil.

An area of a mine (including a self heating spoil pile) was chosen for detailed analysis for each set of data. The area within a particular surface temperature range was calculated for each of the

data sets. As the background surface temperatures depended on the meteorological conditions prevailing at the time of the flight, an area of the mine known not to be self heating was used to normalise the temperatures for the three data sets so that the results could be more accurately compared.

Ground truthing temperature data were also obtained and surface temperature was calculated from the infra-red data sets using calibration curves developed from ground truthing data.

The area as a function of surface temperature for part of a spoil pile was used along with the relationship between greenhouse gas emissions and temperature to calculate greenhouse gas emission rates.

KEY RESULTS AND OUTCOMES

1. The empirical relationship between greenhouse gas emissions and surface temperature was improved

A series of chamber measurements were carried out to establish the relationship between greenhouse gas emissions and the surface temperature of hot spoil. A new aluminium chamber was designed and constructed to allow higher temperature data to be obtained than was possible from ACARP Project C8059. In addition a better method for measuring representative temperatures was developed using a hand held infra-red sensor. The result of improved emission and temperature measurements reduced the uncertainty in the relationship between emissions and temperature compared with the results from ACARP C8059. For example the spread in the data for emission rates at a surface temperature of 50°C has reduced from a factor of ~10 to a factor of ~3.

2. The process of allocating mapping co-ordinates to infra-red pixels requires improvement

The infra-red data supplied during the project were in the form of pixel values with each value corresponding to a temperature. In order to use the data, the pixels had to be aligned with known ground references. A key issue has been the lack of geo-referencing data integral with the infra-red pixel data. As a consequence well-known landmarks were required to orient the infra-red output images. Because of this it was only possible to overlay the temperature maps on the mine contour maps, to within a precision of ~1.5 pixels (for the 7x7m data).

At the time of writing, the infra-red scanner is in the process of being modified to allow GPS data to be obtained simultaneously with the infra-red data. This will greatly facilitate the analysis of future results and make it possible to compare temperatures for particular locations to a higher degree of accuracy than is presently the case.

3. The 2x2m pixel flight provided greater resolution and different area versus temperature distributions compared with the 7x7m pixel flights

Because of the greater resolution of the 2x2 m pixel data, these data showed a different area versus temperature distribution. This was particularly marked in the low to mid range temperatures (17 to 30°C) and for the hotter zones (>50°C) where the 2x2m data apportioned a greater fraction of the area compared with the 7x7m data.

4. The 7x7m pixel data for the same area of spoil pile showed acceptable consistency for the data 1 year apart

While there were differences in the distribution of area versus surface temperature for the data obtained 1 year apart, the results were broadly consistent. However, it is not clear, at this stage, whether the differences between the two data sets reflect real changes or scatter in the data. This can only be resolved by acquisition of further sets of data over a longer period of time.

5. The method of airborne infra-red survey can be used to monitor the general temperatures of the spoil pile

The analysis of the data for the study area shows that the method of airborne infra-red survey can be used to monitor the general temperatures of the spoil pile provided the data are appropriately processed and interpreted. While there was some scatter in the results the method can be used as a broad management tool to monitor changes in spoil heating over time periods consistent with those known to be appropriate from other studies of spoil heating and cooling ie time frames of several years. (Note that this use of airborne thermal infra-red data must be distinguished from previous attempts to use similar data to probe the inner thermal behaviour of spoil piles, an altogether much more difficult, if not impossible undertaking).

6. Greenhouse gas emission calculations showed acceptable consistency between the two 7x7m pixel data sets and increased values for the 2x2m pixel data

The area as a function of surface temperature for the study area was used along with the relationship between greenhouse gas emissions and temperature to calculate greenhouse gas emission rates. These results showed acceptable consistency between the two 7x7m data sets and increased values for the 2x2m data, presumably reflecting the ability of the finer resolution data to see the smaller scale, hotter features.

7. The temperature taken to represent non-heating ground is critical in calculating the total greenhouse emission rate

The value for the total greenhouse emission rate depends critically on the temperature taken to represent non-self heating ground. Consideration has been given to this aspect during the current project, but requires further consideration. This will be explored further in ACARP Project C11023, which has just commenced. Project C11023 will seek to develop a method to use techniques from air quality modelling to back calculate CO_2 emission rates from monitored data on CO_2 concentrations. A feature of the air quality model is that it also calculates surface temperatures and will be used in C11023, along with the CSIRO model of spoil pile self-heating, to examine in greater detail, the variations in surface temperature.

8. The project methodology can be used to monitor total greenhouse emissions

The method developed during this project allows the total greenhouse gas emissions to be estimated and monitored. The data obtained from the 2x2m resolution data provide greater resolution of ground features, which translates into more accurate greenhouse gas predictions. However, the estimates are still subject to uncertainty and may not be accurate enough to be used for reporting purposes. Nevertheless, should the infra-red surveys be flown over a period of several years (as described above) then the method could be used to discern trends in the greenhouse gas emission rates.

TABLE OF CONTENTS

1 INTRODUCTION

1.1 Background

In recent years there has been a growing realisation that spontaneous combustion in coal mines may be a large source of the greenhouse gases CO_2 and CH_4. The Inter-Governmental Panel for Climate Change (IPCC) considered spontaneous combustion as a source but excluded it from the inventory as is was considered that no acceptable method for estimating emissions was available.

In their study for the Australian Coal Association on greenhouse gas emissions from coal mining, Williams et al. (1998), suggested that up to 25 percent of the total emissions from an open cut coal mine with spontaneous combustion in the spoil may arise from spontaneous combustion and low temperature coal oxidation. While the assessment made by these authors represented the "state of the art" at the time, the estimates were based on very limited data and had large associated uncertainty.

In March 1999, ACARP Project C8059 was commenced by the CSIRO Division of Energy Technology (Carras et al, 2000). The overall objective of this project was to provide methods, supported by direct measurement, to quantify the emissions of greenhouse gases from spontaneous combustion in Australian open cut coal mines. Measurements of emissions from spoil piles, coal rejects and tailings were conducted at 11 mines in the Hunter Valley in NSW and the Bowen Basin in Queensland. The results of this work led to the development of emission factors for several broad categories based on the extent of spontaneous combustion present. These were

1) intense spontaneous combustion characterised by smoke and steam, major cracks, surface discolouration and obvious signs of venting;

2) spontaneous combustion with less well pronounced signs, small cracks, surface discolouration and occasional whisps of smoke and steam;

3) no sign of spontaneous combustion.

In addition to these emission factors, an approximate relationship between greenhouse gas emissions as a function of near surface temperature was established.

While Project C8059 significantly advanced the knowledge of emissions from spontaneous combustion in open cut coal mines, there were practical problems in applying the results to estimate greenhouse gas emissions from operating mines. Firstly, while the chamber technique developed in that project provided direct emission measurements, it was labour intensive and required many measurements to obtain representative values. Secondly, it is difficult to assess the extent of spontaneous combustion in spoil piles. While the installation of probes which allow measurement of temperature at depth have been used successfully in the past (Carras et al, 1994,1998), the use of this method to survey a large mine would require very many probes and would be impractical. An alternative approach has been to rely on mine personnel estimating the extent of spontaneous combustion. However, these estimates are by necessity, subjective. To address these limitations, ACARP Project C9062 was developed with the view to using remote sensing techniques such as airborne infra-red thermography to investigate whether more accurate and cost-effective monitoring of the extent of spontaneous combustion in spoil piles and the associated greenhouse gas emissions could be achieved.

While there had been previous attempts to use airborne thermal data to map the extent of spontaneous combustion in open cut mining operations it had generally not found favour with mine personnel because of the perceived difficulty in interpreting the data. However, there have been considerable improvements in both the technology and knowledge of spontaneous combustion in recent years. It is appropriate to reassess this approach to monitoring spontaneous combustion and its potential extension to greenhouse gas determination.

1.2 Objectives

The principal objectives of the project were:

1) to develop a method for estimating and monitoring the extent of spontaneous combustion in open cut coal mines using airborne infra-red thermography and

2) to use the temperature data from the infra-red surveys to estimate greenhouse gas emissions from spontaneous combustion.

2 NATURE OF COAL MINE WASTE DUMPS

Before proceeding to a description of the experimental methods employed in the current project it is necessary to discuss, briefly, the phenomenon of spontaneous combustion and its manifestation in spoil piles. This is critical to the interpretation of the airborne infra-red data.

Low temperature oxidation occurs whenever carbon containing material is exposed to oxygen in the air. At an open cut coal mine this occurs whenever coal, carbonaceous materials such as shales, siltstones and mudstones and waste such as reject and tailings are exposed to air. Research over a number of years has shown that the rate of oxidation for a particular material depends on, among other things, temperature, particle size, oxygen partial pressure, water content and extent of previous oxidation (see eg Carras and Young, 1994). The rate of reaction increases exponentially with temperature but decreases with time of reaction. In other words, the coal 'ages'.

Spontaneous combustion of coal occurs when the low temperature oxidation process referred to above leads to the rate of heat release within a spoil pile being greater than the rate at which heat can escape from the spoil pile. This causes the temperature of the coal to rise significantly leading to combustion. From this point the fire resulting from spontaneous combustion is no different to any other fire in that it requires oxygen, heat and fuel to continue to burn. Spontaneous combustion can occur in any of the

3

carbonaceous materials described above namely in coal stockpiles, spoil piles, reject dumps and tailings.

Figure 1 shows a schematic of a dragline spoil pile illustrating the basic processes leading to heating and the emission of greenhouse gases.
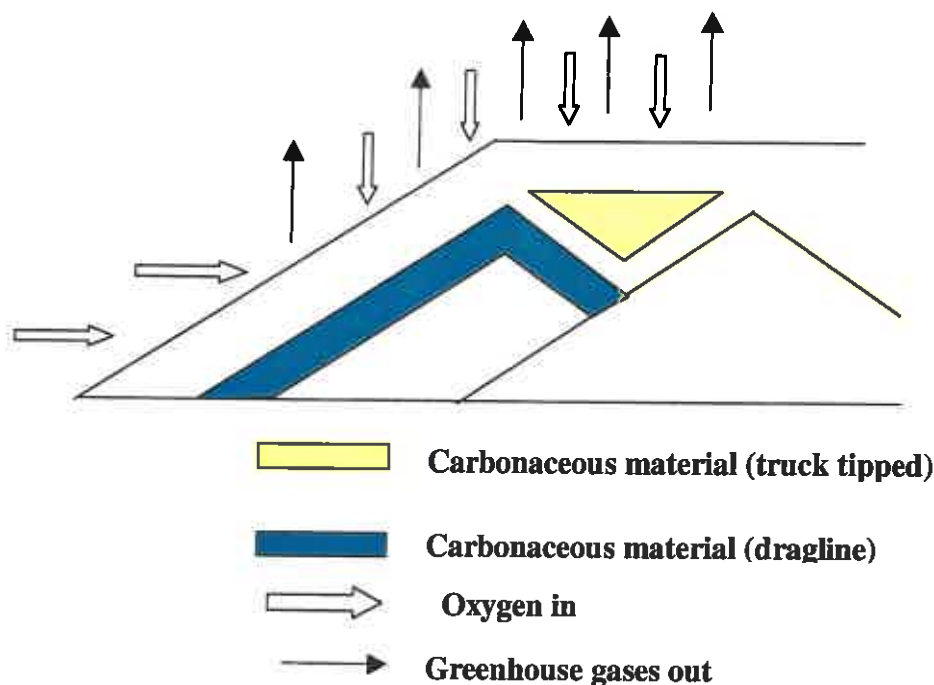

Carbonaceous material (truck tipped)	
Carbonaceous material (dragline)	
Oxygen in	
Greenhouse gases out	

Figure 1 Schematic diagram of spoil pile oxidation and greenhouse gas emissions.

The major manifestation of spontaneous combustion is elevated temperature. However the expression of the temperature at the surface depends on a number of factors including the location of the heating and the thermal properties of the overlaying materials. Consequently complete diagnostic data from spoil pile surface temperatures is not possible. Nevertheless surface temperatures, while not allowing the full extent of spontaneous combustion to be inferred, may be able to be used as a useful management tool for the long term monitoring of spontaneous combustion behaviour. For instance a general decrease in surface temperature over a period of time for an area of spoil will reflect the cessation of self heating following the application of successful control

methods. This more general use of the method must be distinguished from attempts to use surface infra-red data to provide specific data on the location of heating within spoil piles. The latter is not normally possible due to the reasons referred to above.

In addition to the above, the issue of the relationship between the surface temperature expression and the rate of emission of greenhouse gases also requires careful interpretation. Some of the issues are illustrated below. Figures 2 and 3 show two examples of advanced spontaneous combustion which highlight some of the issues which will act to confound attempts to form a relationship between the emission rate of greenhouse gases and the surface temperature of the spoil pile.

**Figure 2 Emissions from unconsolidated spoil material
showing general surface emissions.**

Figure 2 shows a case where greenhouse gases are venting in a more or less uniform manner over a hot surface. In this case the greenhouse gases vent from a relatively high

permeability region and to a first approximation, can be considered to represent a uniform emission over the affected surface.

Figure 3 Emissions from a crack in spoil due to spontaneous combustion.

Figure 3 on the other hand shows a severe crack in a spoil pile with emissions essentially restricted to the crack itself. These cases of surface expression of spontaneous combustion highlight the high level of spatial resolution of the surface temperatures required to capture features such as large cracks.

Data from ACARP project C8059 had suggested that an approximate correlation existed between surface temperature of spoil piles and greenhouse gas emission rate. As part of the current project this correlation has been explored in greater detail and will be discussed subsequently. However, some of the factors that influence the relationship between greenhouse gas emissions and surface temperature are discussed briefly below.

The rate of emission will depend on the location of spontaneous combustion and the nature of the spoil pile surface ie

1) the location of fuels (coal and carbonaceous waste) and hence potential hot zones.
2) the voidage and particle size distribution in the dump which will determine the diffusion coefficient and permeability of the dump.
3) the extent of oxygen transport into the dump which is important (along with temperature) in determining the ratio of CO_2 to CH_4 produced.
4) the presence of cracks in the dump which act as conduits to the surface for the gases produced from spontaneous combustion and low temperature oxidation.

The concentration of oxygen within a spoil pile will depend on the dominant oxygen transport mode and the rate at which oxygen is being consumed. For instance diffusion will restrict appreciable oxygen concentration to within ~10m of the surface whereas forced and natural convection can transport oxygen into the centre of a spoil pile particularly if there are large cracks. The ratio of CH_4 to CO_2 in the gases will depend critically on these physical factors as well as the chemical processes taking place. (Note that the extent of oxygen penetration into a spoil pile, by diffusion, depends on many factors. The value of 10m quoted above is meant to serve as an approximate guide only

as, depending on circumstances, the penetration depth can be much greater, or much less, than 10m).

Different waste piles give rise to different surface structures. For instance dragline or truck spoil (greater than ~15m in thickness), including when it is overdumped by inert material, can form large cracks which act as conduits for the emissions of combustion products including greenhouse gases. Other waste materials, such as coarse reject or block tipped spoil, tend to exhibit less cracking as the materials are generally more homogeneously distributed compared with dragline spoil or spoil tipped over a face.

Large cracks emitting hot gases will tend to dominate the local emissions. Smaller cracks or higher permeability regions will assist to distribute the overall emissions more widely. Consequently, considerable variation in the data is to be expected. This is illustrated schematically in Figure 4 and by the photographs in Figures 2 and 3.
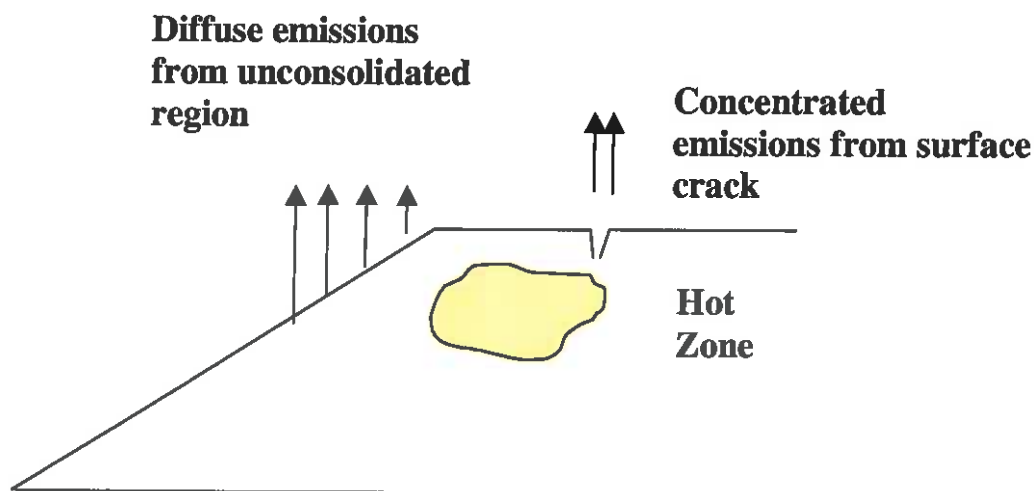
Diffuse emissions from unconsolidated region

Concentrated emissions from surface crack

Hot Zone

Figure 4 Schematic of greenhouse gas emissions from spoil with spontaneous combustion.

The above factors have been taken into account in the development of the relationship between surface temperature and greenhouse emissions and are discussed below.

8

3 EXPERIMENTAL METHOD

3.1 Airborne Infra-red Thermography

Airborne infra-red surveys of the upper Hunter Valley were flown by Air Target Services Pty. Ltd. using a Daedalus 1268 Airborne Thematic Mapper (ATM) system fitted to a Cessna 414A aircraft. The Daedalus is capable of sensing 12 individual wavelength bands from ultra-violet to infra-red. For this work, only the infra-red bands 11 and 12 were used. Wavelengths of 8-14 μm were used for both bands with the gain for one set of data being set to half, to attempt to prevent saturation of the infra-red channels at the highest temperatures.

3.2 Flights and Ground Truth

Two flights were carried out approximately 1 year apart. The first was made in September 2000 between Singleton and Muswellbrook while the second flight was carried out in October 2001 and focussed on a smaller area selected from the area covered by the first flight. Cloudless and windless conditions were sought for each flight as these conditions lead to higher quality data. Windows of opportunity were initially selected on the basis of weather forecasts and a decision to proceed with the flight made late in the day. This made coordination with ground crews difficult due to the 3 hour driving time between the Sydney base and the Hunter mines where ground truthing was carried out. On a number of occasions the flights were abandoned due to late weather changes mainly low level winds and the presence of fog.

Data from the flights were presented to CSIRO as integers representing each of the pixels measured by the airborne scanner. Each pixel had a numerical value with each integer corresponding to a distinct ground temperature and related to the temperature by the calibration function.

At the time of each flight ground level measurements of surface temperature were also carried out in order to provide measurements which could be used to ground truth the aircraft data.

Figure 5 shows part of the region covered by one traverse of the aircraft during the first flight.

Figure 5 Raw infra-red data as received. The area in the image was taken between Singleton and Muswellbrook and covered an area ~5km wide and 40km long.

For the case of Figure 5 above, each pixel corresponded to an area of ~7x7m.

For the second set of flights (October 2001) a smaller region of the Hunter was re-flown at the 7x7m pixel resolution. In addition a further set of traverses at much lower altitude were used to provide a pixel resolution of ~2x2m. (Note that the actual pixel size was slightly less than the nominal value of 2x2m). The aim of this higher resolution data was to check the overall precision of the 7x7m data as the potential significance and influence of cracks in the spoil pile had been highlighted during the course of the project. (This will be discussed in detail in a subsequent Section). A brief summary of the flights carried out is shown in Table 1.

Table 1 Characteristics of the flights.

Date of Flight	Pixel size	Region covered
Sep 2000	7x7m	40 x 20 km zone from Muswellbrook to north of Singleton
Oct 2001	7x7m	Selected 20 x 15 km region in the upper Hunter
Oct 2001	2x2m	Selected 9 x 7 km region in the upper Hunter

3.3   Chamber Measurements

Greenhouse gas emission flux measurements were made using the chamber technique described in the final report for ACARP Project C8059 (Carras et al., 2000). This technique involved placing a purpose-built chamber on the surface of spoil and measuring the concentration of CO_2 and CH_4 inside the chamber with continuous gas analysers located in a 4WD vehicle. Flux measurements were made on a variety of surfaces with or without active spontaneous combustion. Measurement sites were selected so as to provide a wide range of average surface temperatures. The temperatures were measured before dawn to eliminate the effects of solar heating and to replicate the conditions seen by the aircraft. This approach necessitated selecting appropriate sites during the day and returning before dawn the following morning to make the temperature measurements. Flux measurements were generally made later in the day.

The surface temperatures measured under these conditions ranged from about 10 °C (unaffected ground) to more than 300 °C in open cracks. Note that although spot temperatures of more than 300 °C were observed, the mean surface temperature (comprising six or more individual readings) over the chamber area was normally considerably less.

In one area a 20m by 20 m grid was marked out at 2 m spacing and the pre-dawn surface temperature measured at each 2x2m point. The area bounded by this grid was approximately equal to the area represented in the infra-red image by eight of the 7x7m pixels. This area contained a large crack approximately 150 mm wide at its widest point from which hot gas was being emitted. (Note that the gas temperature was more than 300 °C in places). Emission flux measurements were made within the grid area at regular spacings so that about 50 percent of the total area was covered by the chamber.

For areas of spoil where the ground temperature was below about 70 °C the polycarbonate chamber from Project C8059 was used. The polycarbonate chamber was 4 m long by 1 m wide, covering an area of 4 m². The polycarbonate chamber is shown in Figure 6.

Figure 6 Polycarbonate chamber for use with ground temperatures less than 70°C.

One of the limitations of the data obtained during ACARP project C8059 and which was highlighted during the course of the current project was the inability of the chambers constructed of polycarbonate to withstand the high temperatures associated with large cracks in the spoil piles from which large volumes of hot gases could be emanating. In order to overcome this deficiency a new aluminium metal chamber was designed and constructed and used to obtain high temperature data. This chamber had dimensions of 2m x 1m (ie 2m^2) and is shown in Figure 7 after it had been constructed at the CSIRO laboratories at North Ryde.

Figure 7 Aluminium chamber for use with higher temperature emissions.

The method of measurement was the same for both chambers; the chamber was placed over an area of spoil and a steady stream of ambient air was drawn through the chamber at a known rate with a fan attached to one end of the chamber. The purpose of the air flow was to dilute the gas inside the chamber so that the concentrations of CO_2 and CH_4 were maintained within the dynamic ranges of the gas analysers. Typically, the air flow was between about 500 to 1000 L min^{-1}.

Sample air was withdrawn from the chamber through a 6 mm diameter nylon tube by a small diaphragm pump at about 5 L min^{-1} and passed into a polyethylene manifold located inside a specially instrumented 4WD vehicle. The sample air was analysed for CH_4 with a Horiba hydrocarbon analyser (using the principle of flame ionisation detection) and CO_2 with a Leybold Binos 100 non-dispersive infra-red analyser. If

14

necessary, the sample was further diluted to keep the concentrations within the range of the instruments. A laptop computer interfaced to these instruments continuously logged the data.

Emission fluxes were calculated using the following expression after the concentrations in the chamber had attained steady state:

$$F = f_d (C_s - C_a) / A \qquad (2.1)$$

where F is the emission flux, C_s is the concentration of CO_2 or CH_4 in the chamber, C_a is the concentration of CO_2 or CH_4 in the dilution air flowing through the chamber, f_d is the dilution air flow rate and A is the area of the chamber.

Methane has a greenhouse gas effectiveness factor of 21, hence CO_2 equivalent emissions were calculated by multiplying the CH_4 component by 21 and then adding the corresponding CO_2 flux.

3.4   Ground-Truthing Temperature Measurements

Surface temperature measurements were made at a number of sites covered by the aerial infra-red surveys on, or near, the time of the flights. For the first flight in September 2000, pre-dawn ground surface temperatures were measured at three mines. Temperatures were measured on hot ground and also on areas where there had never been any spontaneous combustion.

On the morning of the second flight (October 2001), pre-dawn surface measurements were made in an area of spoil with active spontaneous combustion and associated hot ground. Temperatures were measured within a 7 by 7 m grid (approximately corresponding to one pixel in the low resolution data) at 1 m spacing. As well, temperatures were measured in a variety of areas around the mine site including

unaffected spoil, haul roads, unmined (i.e. vegetated) ground and water in dams. The water temperature in a number of dams outside the mine lease was also measured.

The temperatures were measured with a hand held infra-red sensor and cross checked with a thermocouple probe which had been developed for surface temperature measurement.

4   RESULTS AND DISCUSSION

4.1   Ground Temperatures

Flight No 1 – September 2000

The ground-truthing site at Mine 1 was on the edge of a spoil pile exhibiting spontaneous combustion. The surface temperatures measured at this site ranged from about 10 $^{\circ}$C to 120 $^{\circ}$C and the ambient air temperature was 7 $^{\circ}$C. Some distance away from this site, surface temperatures were measured on an area (50 x 50 m) of hard packed ground which was unaffected by spontaneous combustion. The mean temperature on this section of ground was 7.5 $^{\circ}$C (std dev = 1.41, n = 26).

At Mine 2 the ground temperatures in the spontaneous combustion affected area ranged from about 10 $^{\circ}$C to about 90 $^{\circ}$C. There were no areas near to this site where we could be confident that were not subject to some degree of heating so baseline readings were not obtained at this mine. The ambient temperature was 6 $^{\circ}$C.

Measurements were made at Mine 3 on spoil adjacent to probes which had been previously placed by CSIRO for monitoring spontaneous combustion. The range of surface temperatures at this site was 14 to 57 $^{\circ}$C. Baseline temperatures were measured several hundred metres back from the edge of the spoil pile. This is an area which is known to have had no spontaneous combustion (from probe data). Here, the mean temperature was 9.9 $^{\circ}$C (std dev = 0.99, n = 8).

Flight No 2 – October 2001

During flight 2 detailed measurements were carried out at a number of locations. Figure 8 shows the temperatures measured on the ground for one area measuring 7x7m during the second flight. The data have been contoured and are presented as isotherms.
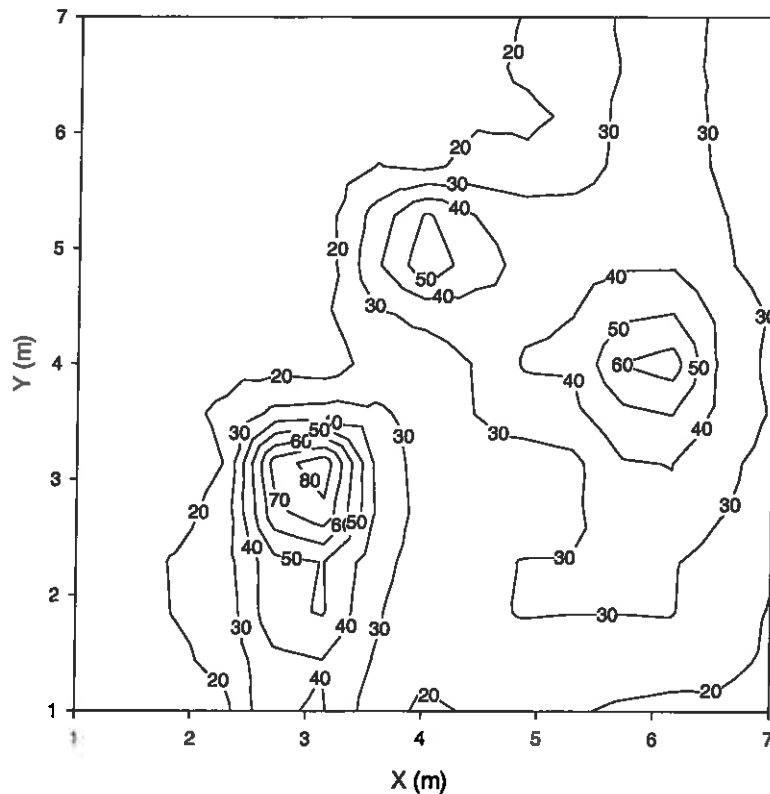

Figure 8 Example of temperature contours on 7 x 7 m grid on hot ground during second flight.

In this region, the temperatures varied from about 12 to 90°C and the ambient temperature was 11.5 °C. The average temperature for the region was 25.3°C (number of measurements, n =49).

The temperature of unaffected ground around the mine, which included bare ground, haul roads and vegetated ground averaged 14.1°C. (Note that the range of values was from 12.5 to 15.5°C). The temperature of water in dams was very consistent, averaging 19.1°C (n = 4).

It was originally intended to use the ground-truthing measurements to compare with the temperatures provided by the aerial infra-red data on a pixel by pixel basis. As it turned out, however, this proved to be impractical. This was because the infra-red data did not contain any geo-referencing information and could not be referenced to ground features with the required degree of precision for this to be achieved. Consequently, we were unable to identify the ground-truth sites on the infra-red images with sufficient accuracy (i.e. to within one pixel or 7 m) to directly compare the particular pixel values with the measured ground temperature. Despite this, the average ground temperatures of the unaffected ground and water temperatures of dams could be used for comparison and were used as the major calibration method.

As will be seen subsequently the issue of ground truthing is important in setting the appropriate values for the infra-red data.

4.2   Emission Fluxes

As discussed above, data from ACARP project C8059 had suggested that an approximate relationship existed between greenhouse gas emission rate and surface temperature of the spoil. While it was well recognised that many factors would act to obscure such a correlation (see Section 2) it was considered that a useful correlation could nevertheless be obtained for these purposes.

Spatial Variability of Temperature and Emission Fluxes

To establish the variability of emissions and temperature over the area represented by individual pixels in the infra-red data, measurements were carried out at close spacings

within an area (which contained a crack issuing hot gas) of approximately 20 x 24 m. This experiment was performed before the high-temperature aluminium chamber was built so measurements of emissions from the hottest parts of the area, were not made. Nevertheless, a large proportion of the area was characterised.

The range of temperatures and average emission fluxes measured within this area is shown in Table 2 .

**Table 2 Range of temperatures and emission fluxes
for a 20x24m section of spoil surface.**

	Temperature ($^{\circ}$C)	CO_2 Equivalent Emission Rate (kg/m^2/yr) averaged over the chamber area
Minimum	8	3.9
Maximum	330	1895
Mean	22.1	371
Std Dev	37.1	452

(Note that the temperatures in Table 2 show the range encountered over the areas covered by the chamber and that the emission rates are averages over the area of the chamber containing the temperature reading).

It is apparent from these figures that there was a high degree of variation in both temperature and emission flux over this relatively small area. The data have also been plotted as contour maps in Figure 9 to more clearly show this variation.
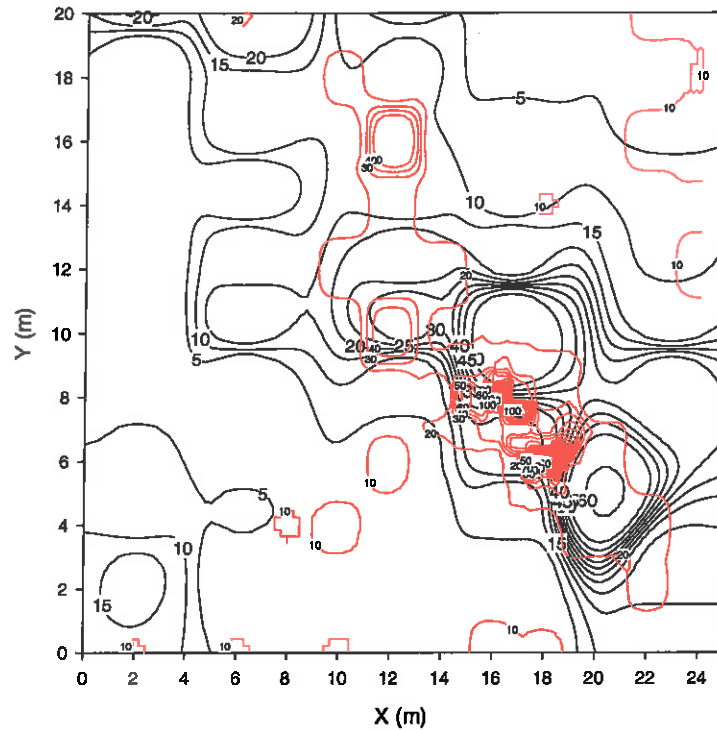
**Figure 9 Plot of surface temperature and emission rate for a
20x24m section of spoil.**

The temperature (red line °C) and emission flux (black line kg/m^2/yr) contours are closely aligned and follow the crack which passed through the measurement site. The hottest part of the crack was a section about 6 m long with each end having the approximate grid coordinates of 16,8 and 20,4. The contour plots clearly show that this is the region of highest temperature and emission flux.

The lack of geo-referencing data with the thermal image prevented direct comparison on a pixel by pixel basis of these temperatures with the corresponding pixels in the infra-red data.

Emission Flux – Temperature Relationship

Figure 10 shows all of the data plotted as CO_2 equivalent emission rate as a function of average surface temperature with the line of best fit also shown.
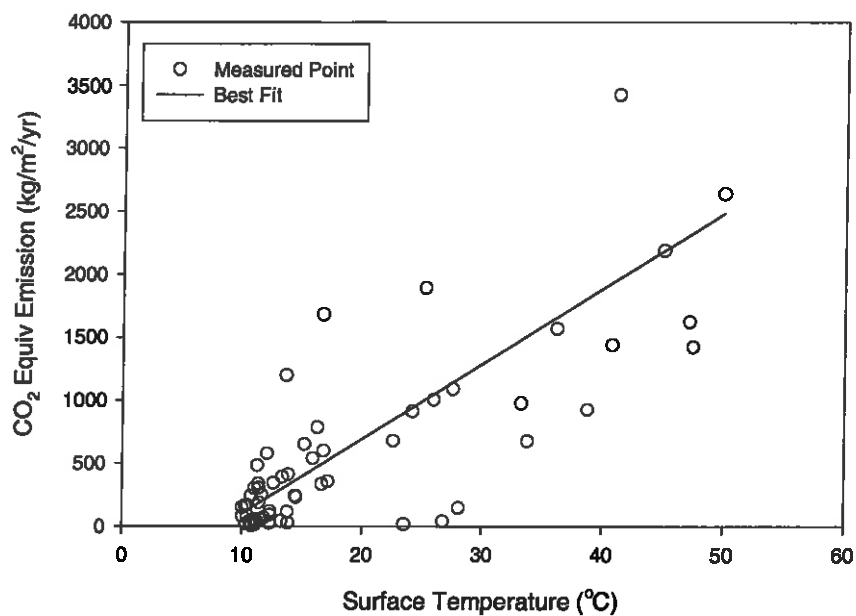

Figure 10 Measured average emission rates (as CO_2 equivalent) as a function of average surface temperature. The solid black line is the line of best fit.

Compared to the data reported in Project C8059, the results plotted in Figure 10 show considerably less scatter. For instance, for an average surface temperature of 50°C the scatter has reduced from a factor of ~10 (ACARP C8059) to a factor of ~ 3. There is, however, still considerable variability in the data, particularly for the surface temperatures below ~ 30 °C.

The emission measurements showed (Figure 10) that negligible greenhouse gas emissions were measured when no spontaneous combustion was present and for surface temperatures of up to ~15°C. On the other hand when spontaneous combustion was present at 18 °C the rates could be as large as 1700 kg/m^2/yr. The data in Figure 10 also indicate that the surface temperature below which significant emission rates were not measured (when there were no hot cracks present) was about 14°C. The above give rise to some uncertainty at the lower temperature end as the value of surface temperature measured when there is no spontaneous combustion depends also on the ambient meteorological conditions. This issue requires further consideration and will be explored further in ACARP Project C11023, which has just commenced. Project C11023 will seek to develop a method to use techniques from air quality modelling to back calculate CO_2 emission rates from monitored data on CO_2 concentrations. A feature of the air quality model is that it also calculates surface temperatures and will be used in C11023, along with the CSIRO model of spoil pile self-heating, to examine in greater detail, the extent of variation in the surface temperature. Further measurements of the emission fluxes may then be required to better define the lower temperature end of Figure 10 and if this proves to be the case, will be carried out as part of project C11023. However, as a result of the issues raised in Section 2 concerning the nature of emissions from spoil surfaces it is unlikely that making additional measurements of temperatures and emissions will reduce the scatter in the data at the higher temperature end beyond that achieved by the above results. Consequently, the scatter in the data in Figure 10 will be reflected in the calculated greenhouse gas emission values.

4.3 Airborne Infra-red Data

Before moving to the results of the infra red surveys, it is important to consider some of the uncertainties that can impact on the accuracy of the inferred surface temperature estimates using long wave infra red spectrometers. The spectrometer used in the current study detects the radiation in the selected wave length band emitted from the surface and

also by atmospheric components such as water vapour and CO_2 in the line of sight modified by the atmospheric transmittance.

At night-time, when there is no effective incoming or down welling radiation, the radiation measured by the airborne sensor, has no reflected component and is thus dependent on the thermodynamic temperature of the surface and its emissivity. Emissivity is wavelength dependent and reflects the nature of the emitter. Thus different substances have different emissivities, and hence for a given thermodynamic temperature will have a different radiant or apparent temperature.

Emissivities in the thermal infra red band 8-14 μm have been provided by Salisbury and D'Aria (1992) for a range of substances using field and laboratory techniques. Coll et al, (2002) have derived emissivities from a combination of airborne surveys and ground-based measurements. Emissivity of bare soil was found to be about 0.96, whereas that of cereal type vegetation was 0.98 to 0.99 and water was close to 1. Senescent foliage fell to near 0.9. The impact these differences might have on the apparent temperature can be assessed from Stefan's law (the radiance is proportional to T^4). An object with an emissivity of 0.96 (bare soil) and a temperature of 10°C will appear about 1.5°C cooler than grass with an emissivity of 0.98 and nearly 3°C cooler than a water surface at the same actual temperature. This is consistent with the results of Peck and Lacombe (2001) who measured the night-time thermal contrast of a human against backgrounds of snow, grass and bare soil, with bare soil giving the best contrast. It is apparent that without a detailed knowledge of land cover, one cannot discriminate surface temperatures for the bulk of the surface to better than about 3°C.

Finally, it takes time for the surface heating due to (daytime) insolation, to die away. Soil temperatures can reach high temperatures in strong sunlight (>50°C). Typically, by midnight or a little after, the surface components come to an equilibrium temperature (Peck and Lacombe, 2001). The airborne surveys were carried out after this time and before sunrise.

The following two photographs (Figure 11) show examples of the apparent surface temperature map for two regions of spoil piles containing spontaneous combustion. The pixel values have been converted to surface temperature using the calibration data developed from the ground truthing data and these have been colour coded for purposes of comparison. Note that the temperatures chosen have been done so to demonstrate the broad features of the data. It is possible, however, to consider the temperature data in much finer detail.

Figure 11a shows the apparent surface temperature distribution for a small section of heating spoil.
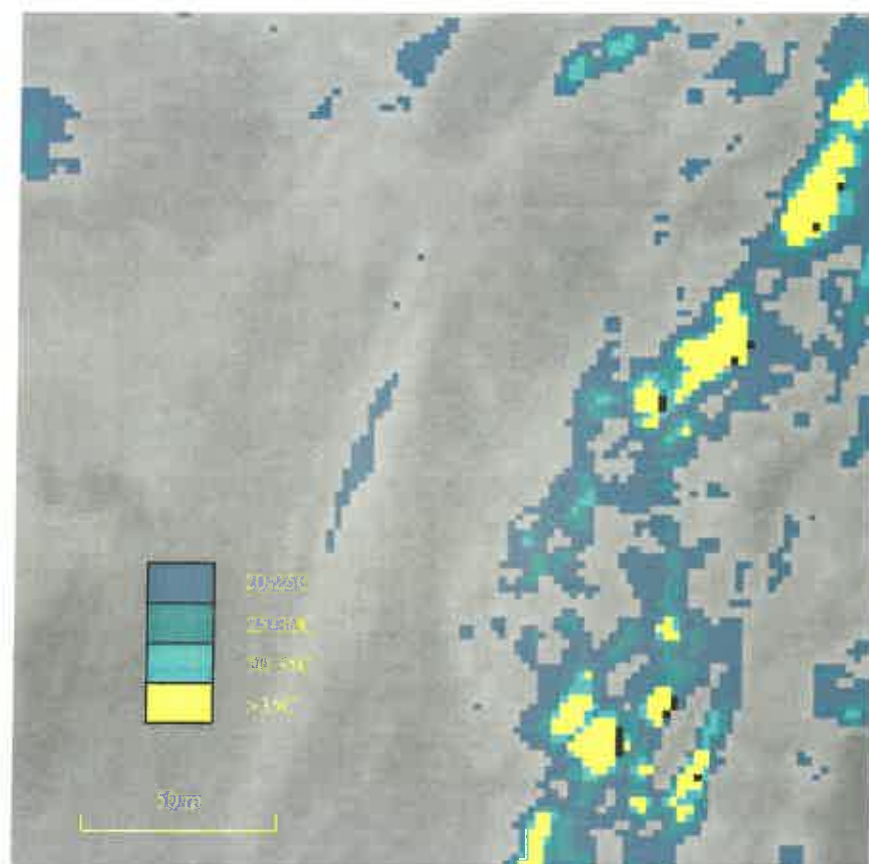

Figure 11a   2x2m pixel resolution for a small self-heating spoil pile

In Figure 11a each individual pixel has been colour coded to reflect the apparent surface temperature.

Figure 11b shows similar data as for Figure 11a, for a different section of spoil, but on this occasion contoured to represent the data as isotherms.
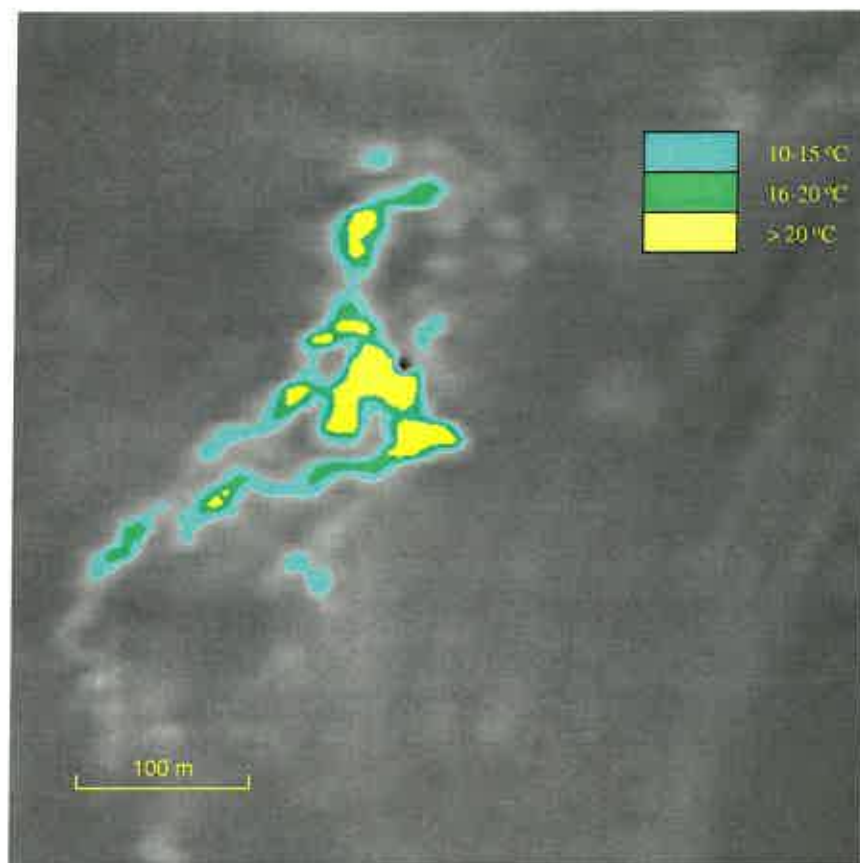

Figure 11b   Isotherms developed from the 2x2m pixel resolution data

Figure 12 shows typical sets of data obtained for the flights of September 2000 and October 2001. The pixel values have been converted to surface temperature using the calibration data developed from the ground truthing data and these have been colour coded for purposes of comparison.
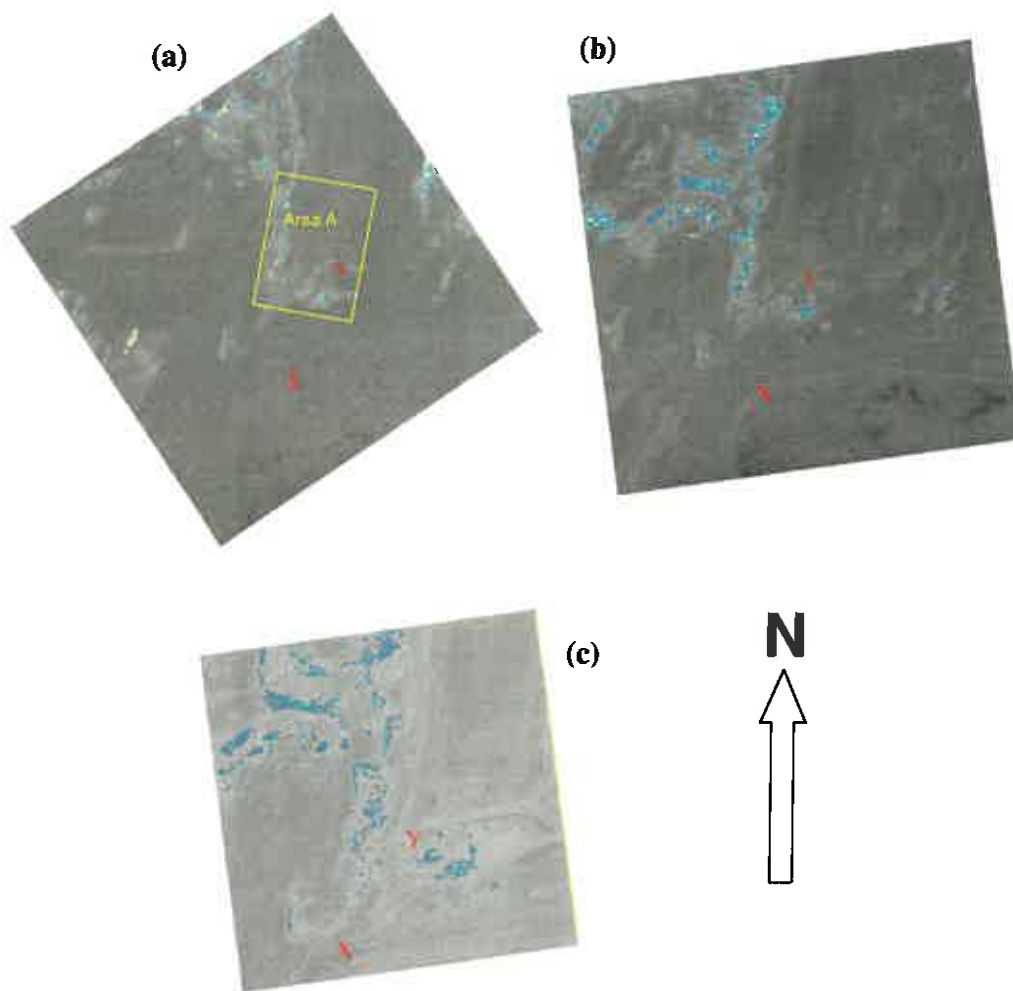

**Figure 12 Colour enhanced infra-red images of spoil with spontaneous combustion.
(a) Flight No 1 (Sep,2000) at 7x7, (b) Flight No 2 (Oct, 2001) at 7x7, (c) Flight no 2
(Oct, 2001) at 2 x 2 m resolution. Points marked X and Y are the same locations in
each image.**

Each of the flights traversed the same section of the mined area but on a different flight path. The thermal pictures have been rotated to align them with each other and at approximately the same scale. Also the clearer image in the bottom picture reflects the greater resolution available from the smaller pixel size for approximately the same area of ground. Two features have also been marked 'X' and 'Y' to allow comparison between the three pictures.

There are clear similarities in the three sets of data displayed in the photographs. There are however some differences between the data from the September 2000 and October 2001 flights. The areas affected by high surface temperatures have changed in both size and location partly, at least, as a result of mine development. There also appears to be a change in the area at the lower temperature end. As already noted, the apparent surface temperature depends on a number of factors that include the local emissivity of the different materials comprising the spoil as well as the meteorological conditions existing at the time of and prior to the airborne data being obtained. These variations are important in ascribing values to the temperature of the background.

Also shown in Figure 12 is an area marked 'A' which was one of a total of four areas chosen from the total data set for more detailed analysis. Area A was used to provide a comparison between the results from the three flights ie the 7x7m pixels from September 2000 and the 7x7m and the 2x2m pixels from the flight of October 2001. This was done by calculating the fraction of the total area, within Area A, for each of the three sets of data as a function of temperature. However, as the background temperature for the flights 1 year apart was different, a method had to be developed to allow for this difference. This was done by matching the lower temperature end for each data set, in a region known to have no spontaneous combustion and then normalising the temperature scale between data sets. This allowed the data obtained approximately one year apart to be compared directly.

4.4   Area Versus Temperature for a Section of Spoil Pile

A plot of area as a function of temperature for Area A is shown in Figure 13.
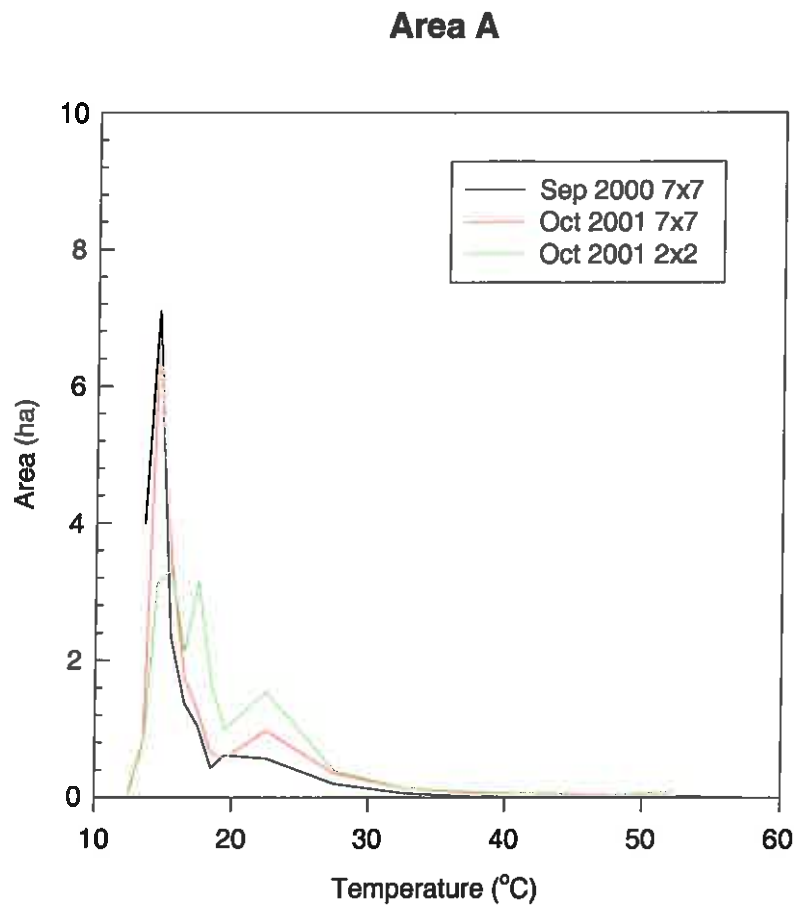
Area A

Figure 13 Area as a function of spoil temperature.

Notice that the data in Figure 13 show quite good agreement for the 7x7m pixels for the two flights 1 year apart. The data for the 2x2m pixels suggest a different distribution of area as a function of temperature particularly at temperatures less than ~25°C. Presumably this reflects the ability of the greater resolution from the smaller pixels to see finer temperature detail than the 7x7m flights.

There are further differences in the data at the larger temperature end. These become more apparent when the data are plotted on a logarithmic scale as shown in Figure 14.
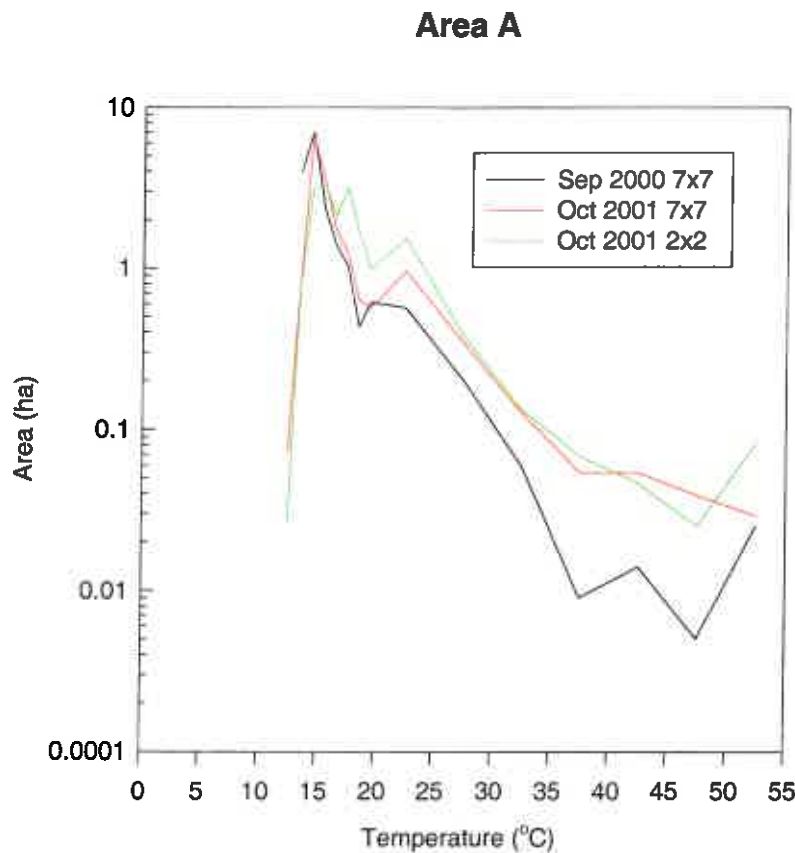
Area A

Figure 14 Plot of area at a given temperature for Area A shown in Figure 12.

The data in Figure 14 show some interesting features. For the two flights at 7x7m pixel resolution the results are very similar for temperatures less than 20°C. There is however a difference in the data for higher temperatures. In the temperature range 20°C to 30°C the area recorded by the second flight is about a factor of 1.5 larger than for the first flight. This ratio increases in the range between 30°C and 50°C where in one case it is as large as a factor of 6. However the areas associated with these largest discrepancies are in fact relatively small (~ 400m^2) and do not make a major contribution to the total area of the

region in question. While these changed area temperature distributions between the 7x7m data, 1 year apart, may be reflecting an increase in heating in the spoil piles, given the relatively small areas it may also be reflecting the general precision of the overall approach.

The comparison between the data obtained for the two flights of October 2001, using the small and large pixel sizes, shows very good agreement in the 30°C to 45°C temperature range, but diverges at the high temperature end. This presumably is reflecting the ability of the 2x2m data to discern cracks at the higher temperature end.

Figure 15 shows a plot of the cumulative area for the mine region as a function of surface temperature for the data from the two flights and for the two different pixel sizes. Each column represents the total area for temperatures greater than the specified value. For instance the entire Area A was at a surface temperature greater than 10°C so the area specified by the column graph at 10°C is the total area of Area A.
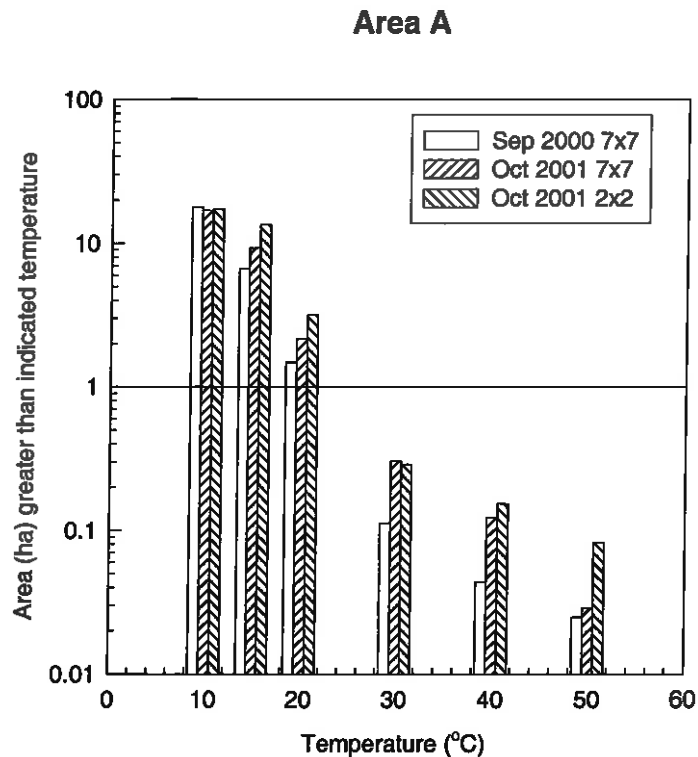
Area A

**Figure 15 Cumulative area for spoil for temperatures
greater than the indicated value.**

A number of features are immediately evident from Figure 15. One is that the total area
for surface temperature greater than 20°C is similar for each of the two flights for the
7x7m pixels with the data for October 2001 being larger than for September 2000. This
trend continues for the areas at temperatures greater than 30, 40 and 50°C. The 2x2m data
follow a slightly different trend. These, generally give larger areas at the higher
temperatures than do than the 7x7m data. This is most pronounced for the 50°C data
where the 2x2m data are about a factor of 3 greater than for the 7x7m data. The change in
the area probably represents differences in the true temperature distribution because of the
greater resolution available from the 2x2m pixel data.

The data obtained from the two flights show that the methodology developed can be used to monitor the extent of heating in an open cut coal mine provided care is used in the interpretation of the data. One of the difficulties with the current data has been the lack of associated GPS information integral with the infra-red data. While this has meant that it has been difficult to align the images with mine maps with great precision, it is clear from Figures 14 and 15 that useful data has still been obtained and that this approach provides a basis for monitoring the extent of spontaneous combustion in spoil piles. However, as only two sets of data have been obtained (ie at an interval of ~13 months apart) it is not possible to assess the extent of scatter in the data. Given the time scales for the cooling or heating of spoil piles, the full meaning of the data shown in Figures 14 and 15 will only become apparent over a period of several years of monitoring.

4.5   Greenhouse Gas Emissions

The data from Figures 14 and 15 have been used along with the relationship between emission rate and surface temperature shown in Figure 10 in order to calculate greenhouse gas emissions. The inferred greenhouse gas emissions are shown in Figure 16 for Area A as a function of surface temperature for the data from the two flights and for the two different pixel sizes.
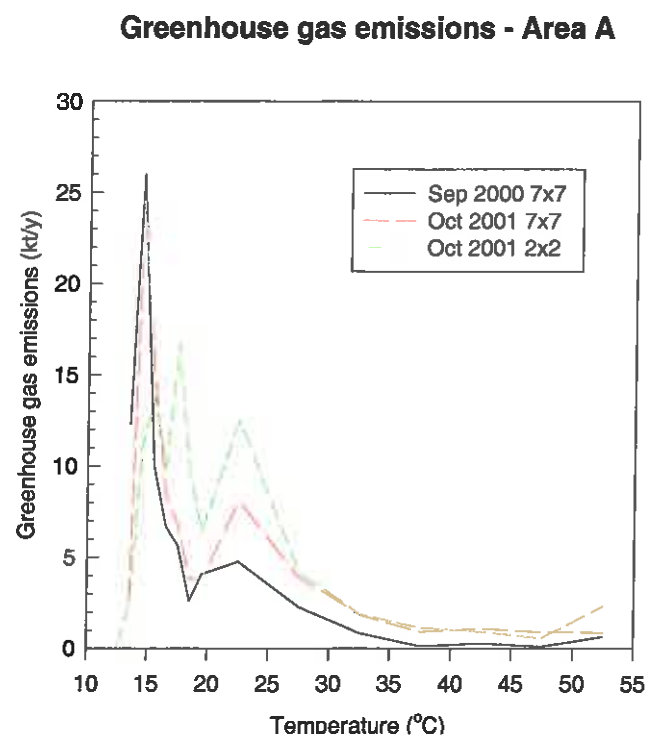
Greenhouse gas emissions - Area A

Figure 16 Greenhouse gas emission rate for a section of a mine.

32

The emissions from the two sets of data for the 7x7m pixels, while in reasonable agreement, suggest an increase in greenhouse gas emissions for temperatures greater than 20°C. This may reflect an actual increase in heating of the area during the elapsed 13 month period between the two flights. However, further data over a longer time period would be required for such a trend to become clear.

Figure 17 shows the cumulative emissions for the same spoil pile for the three different sets of data.
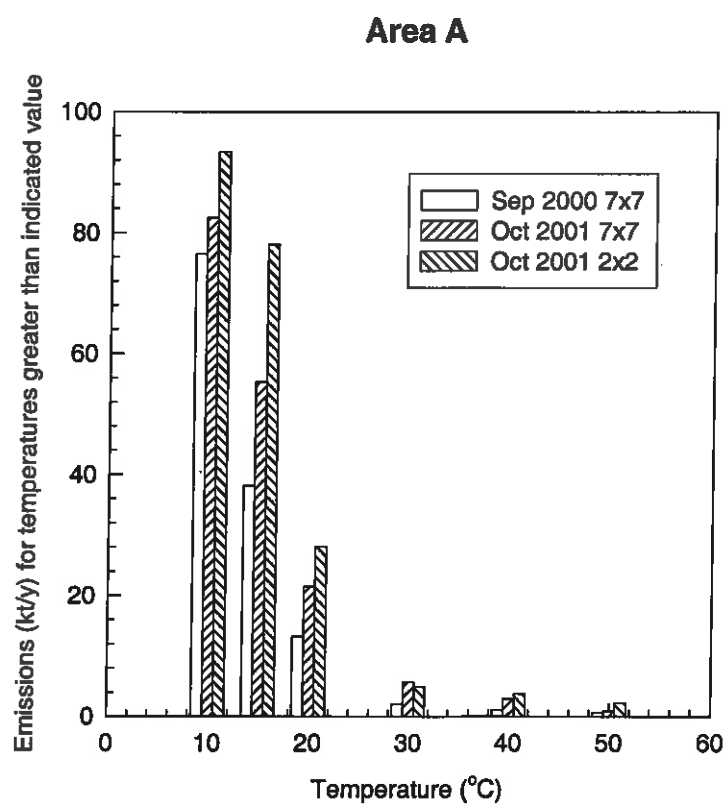

**Figure 17 Cumulative emissions of greenhouse gases
as a function of cut-off temperature.**

From Figure 10 it was shown that for some surface temperatures at 10°C, there were no contributions to the total emissions due to self-heating. However, the line of best fit developed from Figure 10 attributes emissions to these low temperature values. As a surface cut off temperature of 10°C covers all of the Area A (Figure 17), this value of the temperature cut-off will give rise to the largest value for total greenhouse gas emissions. As the temperature cut-off value increases the total greenhouse gas emissions reduce. This is because even though the emissions rates associated with higher temperatures are quite large the high temperature zones represent a small fraction of the total area. On the other hand Figure 17 shows that the emissions associated with the ground at temperatures close to the background values show the largest contribution to total greenhouse gases.

The values of the data are also shown in Table 3.

Table 3 Greenhouse emissions as a function of cut-off temperature.

Temperature (°C)	7 x 7, 2000		7 x 7, 2001		2 x 2, 2001	
	Area (ha)	GHG (kt/y)	Area (ha)	GHG (kt/y)	Area (ha)	GHG (kt/y)
>10	17.8	76.5	16.8	82.5	17.4	93.3
> 15	6.7	38.2	9.3	55.3	13.4	78.0
>20	1.5	13.2	2.2	21.5	3.2	28.0
>30	0.11	2.1	0.30	5.7	0.29	4.9
>40	0.04	1.1	0.12	2.9	0.15	3.8
>50	0.02	0.6	0.03	0.9	0.08	2.3

A comparison between the values of greenhouse gases for the temperature cut-off values of 15°C and 20°C gives a ratio of 38.2 to 13.2 (which is a factor of 2.9) for the first flight and 7x7m pixels, 55.3 to 21.5 (factor of 2.6) for the October 2001 7x7m pixels and 78 compared with 28 (a factor of 2.8) for the October 2001 2x2m pixel data.

From the above data it is clear that the precise value to be associated with 'background' is crucial in determining the total greenhouse gas emissions for a spoil pile. This aspect is considered further in the next Section.

4.6   Issues requiring further consideration

4.6.1   7x7m versus 2x2m pixels

The aim in using the 2x2m pixels was to establish whether the finer resolution provided by this size range was necessary given the cost associated with the increased flight time and data processing required. As is clear from the data in Figure 13, the 2x2m data provided finer resolution, which produced different area versus temperature curves than did the coarser 7x7m data. Attempts were made to explore whether the results obtained from the set of 2x2m measurements made in the current study could be further analysed to develop a more general methodology for future use. This was also based on the fact that chamber measurements that were used to determine the emission flux as a function of temperature had a footprint of 2-4 m^2, similar to the 2m x2m resolution flights.

Three areas, in addition to Area A, were analysed in greater detail. One of these was similar in size to Area A and is referred to as Area B, the second was approximately the area of the whole photographs in Figure 12 (Area C) and the third was a similar sized large area adjacent and to the west of the second area (Area D).

Lack of geo-referencing meant that specifying the target areas in the high and low resolution data could not be done with great precision, as indicated in Table 4 which shows a comparison of the calculated area for each of the areas analysed.

**Table 4 Comparison of estimates of total area using 7x7m pixels
and 2x2m pixels for three different areas of spoil**

Target sites	Area (hectares)		Difference
	High resolution (2m x 2m)	Low resolution (7m x 7m)	Mean and Deviation (%)
Site B	14.5	12.5	13.5 (ha) ±7%
Site C	96.1	85.4	90.8 (ha) ±6%
Site D	82.7	88.4	85.6 (ha) ±3%

The results show that the total area could be determined to within a precision of ~±7%.
Comparison of the percentage areas of ground within a certain temperature range is
shown in Table 5 for each of the three extra areas.

**Table 5 Percentage area of ground within a certain temperature range
for each of the three sites described in Table 4**

Temperature range	Site B		Site C		Site D	
	2m x 2m	7m x 7m	2m x 2m	7m x 7m	2m x 2m	7m x 7m
< 17	65.16	93.15	59.76	91.96	85.80	98.66
17-20	21.56	2.27	20.88	3.27	9.54	0.61
20-25	8.32	2.15	12.11	2.33	3.47	0.28
25-30	2.45	0.86	3.62	1.34	0.60	0.16
30-35	0.94	0.47	1.58	0.53	0.23	0.18
35-40	0.47	0.39	0.73	0.29	0.12	0.07
40-45	0.32	0.39	0.47	0.15	0.07	0.05
45-50	0.14	0.04	0.22	0.04	0.04	0.28
50-55	0.17	0.16	0.19	0.03	0.04	0.11
55-60	0.12	0.04	0.12	0.03	0.02	0.17
> 60	0.36	0.08	0.32	0.03	0.07	0.06

It can be seen from Table 4 that there is proportionately greater areas of hot ground
detected by the 2x2m resolution survey. This was also observed for the data from Area A

(see Figure 13). From Table 5, it can be seen that the low altitude, higher resolution, flights saw significantly more ground with slight heating than the higher altitude 7x7m surveys. It is worth checking whether this is physically possible. This can be done by considering that there are about 16 2x2m pixels for every one 7x7m pixel. (Note as stated previously the nominal 2m x 2m pixels areas are actually slightly smaller than 2x2m). The radiance, R_7, of a 7m x 7m area of ground is given by:

$$R_7 = \sum_{16} \varepsilon_i T_i^4$$

Then the temperature of the 7m pixel will be given by

$$\left[\sum_{16} \varepsilon_i T_i^4 \right]^{1/4}$$

The lower cut –off temperature for one of the temperature ranges was 17°C. For 2 small pixels with a temperature of 13.5°C (background) and 14 at a temperature of 17.4°C, the average temperature of the large pixel will be 16.9°C. For a 7m x 7m pixel with a higher temperature range, the higher resolution pixels could fall into more than two temperature ranges. Thus the results from Table 5 are realistic.

The data in Table 5 can be further analysed by forming the ratio of the 2x2 to the 7x7 areas. The results are shown in Table 6 and plotted along with the data from Figure 13 for Area A, in Figure 18.

37

Table 6 Ratio of the areas within each temperature range for the 7x7m survey compared with the 2x2m survey.

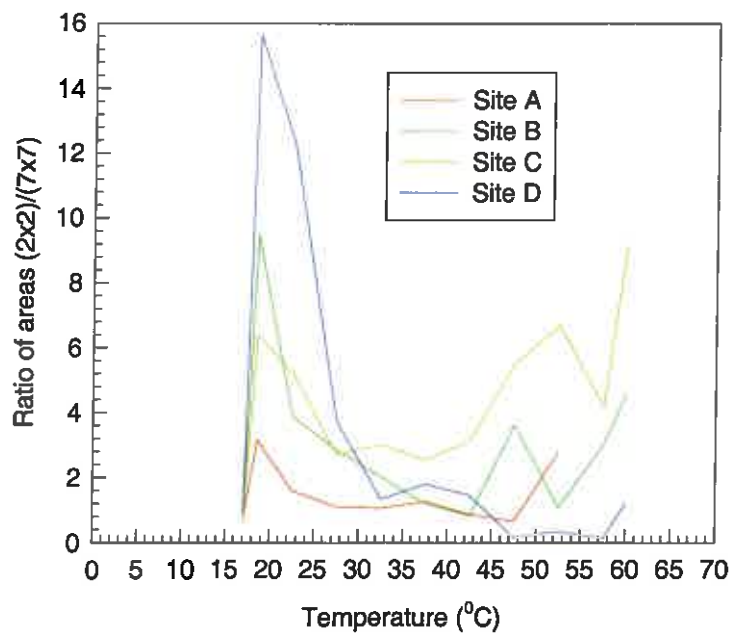| Temperature range	Site B	Site C	Site D
< 17	0.70	0.65	0.87
17-20	9.49	6.38	15.66
20-25	3.86	5.20	12.30
25-30	2.85	2.70	3.72
30-35	2.00	3.00	1.32
35-40	1.19	2.55	1.79
40-45	0.81	3.13	1.45
45-50	3.62	5.49	0.14
50-55	1.06	6.69	0.34
55-60	3.01	4.17	0.12
> 60	4.59	9.17	1.21

Figure 18 Plot of the ratio of areas in a given temperature range for the 2x2m and the 7x7m data sets for the four Areas A to D

The data in Figure 18 show that there are large variations in the ratios from the four different areas. This is because the ratios reflect the temperature distributions of the actual surfaces and are unique for each surface. The spread in the data in Figure 18 is too large for factors to be developed that could form the basis for a more generalised procedure in the manner proposed. Consequently the finer resolution available from the 2x2m pixels serves to increase confidence in the area distribution as a function of temperature.

4.6.2 Emissions from ground at the background temperature

The issue of what constitutes background unaffected temperature is crucial in determining the real greenhouse gas emissions from a heating area and requires further consideration. Based on the discussion in Section 4.3 we consider the cut-off to be about 3-4°C above pre-dawn ambient temperatures. We have used 3.5°C in this report. However, this issue requires further consideration and will be explored further in ACARP Project C11023, which has just commenced. Project C11023 will seek to develop a method to use techniques from air quality modelling to back calculate CO_2 emission rates from monitored data on CO_2 concentrations.

In addition to emissions from ground with surface heating, it is also important to account for emissions from spoil surfaces that are close to or at ambient temperature. (Note that this should not be confused with the small emission rate from biological activity, quantified during Project C8059). The chamber measurements indicated emissions from some such surfaces with no measurable temperature elevation. One approach would be to express the emissions from these cool surfaces as a proportion of the emissions from the surfaces with heating. This would provide a means for attributing background emissions between mines where there is no spontaneous combustion (and the high background emissions of Figure 10 clearly should not apply) from mines where there is spontaneous combustion and the higher background values should be used. A basis for doing this would be to consider the amount of carbonaceous material dumped in the spoil piles, which is a function of the geology of the mine and mining practice, and form the ratio of

the background emissions accordingly. However, how well such an approach would work in practice, needs to be determined.

5   CONCLUSION

The main conclusion to be drawn from this project is that airborne infra-red data can be used to monitor the long term behaviour of spoil piles subject to spontaneous combustion. The same data can also be used to estimate greenhouse gas emissions for spontaneous combustion. However, due to the complexity of the processes involved in producing heating and its surface manifestation and the associated emissions of greenhouse gases the emissions estimates will be subject to significant uncertainty. Whether the uncertainty associated with the greenhouse gas estimates is too large for these values to be used for reporting purposes requires further consideration. Nevertheless (and the expected scatter in the data notwithstanding) over a suitable time period the method could be used to monitor the progress of spontaneous combustion in spoil piles and associated emission of greenhouse gases.

6   ACKNOWLEDGEMENTS

7   REFERENCES

Carras, J.N. and Young, B.C. (1994) Self-heating of coal and related materials: Models applications and test methods. Progress in Energy and Combustion Science, 20, 1-15.

Carras, J.N., Maitra, A., Roberts, O.C., Saghafi, A. and Szemes, F. (1998) The self heating of spoil piles from open cut coal mines. Vol 1 – A field trial of fly ash grouting and an assessment of cover materials. ACARP C3055, pp 157.

Carras J. N., Day, S. J., Saghafi, A. and Williams, D. J. (2000) Measurement of greenhouse gas emissions from spontaneous combustion in open cut coal mines. CSIRO Energy Technology Investigation Report CET IR 333R. ACARP Project C8059 Final Report.

Coll C., Caselles V., Rubio E., Sospeda F. and Valor E. (2002) Temperature and emissivity separation from calibrated data of the Digital Airborne Imaging Spectrometer. Remote Sensing of Environment, 79, 250-259.

Gupta, R.P. and Prakash, A. (1998) Reflectance aureoles associated with thermal anomalies due to subsurface mine fires in the Jharia coalfield, India. Remote Sensing,. 19, No. 14, 2619-2622.

Peck L and Lacombe J. 2000. Predicting variation in thermal infrared intrusion detection. www.dtic.mil/ndia/security2/peck.pdf

Prakash, A. and Gupta, R.P. (1998) Land-use mapping and change detection in a coal mining area – a case study in the Jharia coalfield, India. Remote Sensing, 19, No. 3, 391-410.

Prakash, A., Gupta, R.P. and Saraf, A.K. (1997) The Landsat TM based comparative study of surface and subsurface fires in the Jharia coalfield, India. Remote Sensing, 1997, Vol. 18, No.11, 2463-2469.

Salisbury J.W. and D'Aria D.M. 1992. Emissivity of terrestial materials in the 8-14 μm atmospheric window. Remote Sensing of Environment, 42, 83-106.

Williams. D.J., Carras, J.N., Mallett, C., Mark, M., Cooke, D. and Randall, C. (1998) Scoping Study on the Management and Abatement of Greenhouse Gas Emissions. Report to ACARP . CET/IR46.